Non-equilibrium umbrella sampling applied to force spectroscopy of soft matter

Y. X. Gao, G. M. Wang, D. R. M. Williams, Stephen R. Williams, Denis J. Evans et al.

Related Articles

Deflection of rotating symmetric top molecules by inhomogeneous fields
J. Chem. Phys. 135, 084307 (2011)

A Zeeman slower design with permanent magnets in a Halbach configuration
Rev. Sci. Instrum. 82, 063115 (2011)

Surface-electrode ion trap with integrated light source
Appl. Phys. Lett. 98, 214103 (2011)

Time-dependent manipulation of ultracold ion bunches
J. Appl. Phys. 109, 033302 (2011)

Painlevé singularity structure analysis of three component Gross–Pitaevskii type equations
J. Math. Phys. 50, 113520 (2009)

Additional information on J. Chem. Phys.

Journal Homepage: http://jcp.aip.org/

Journal Information: http://jcp.aip.org/about/about_the_journal

Top downloads: http://jcp.aip.org/features/most_downloaded

Information for Authors: http://jcp.aip.org/authors

Non-equilibrium umbrella sampling applied to force spectroscopy of soft matter

Y. X. Gao,[1] G. M. Wang,[1] D. R. M. Williams,[2] Stephen R. Williams,[1] Denis J. Evans,[1] and E. M. Sevick[1,a)]

[1]*Research School of Chemistry, The Australian National University, Canberra, ACT 0200, Australia*
[2]*Research School of Physical Sciences and Engineering, The Australian National University, Canberra, ACT 0200, Australia*

Physical systems often respond on a timescale which is longer than that of the measurement. This is particularly true in soft matter where direct experimental measurement, for example in force spectroscopy, drives the soft system out of equilibrium and provides a non-equilibrium measure. Here we demonstrate experimentally for the first time that equilibrium physical quantities (such as the mean square displacement) can be obtained from non-equilibrium measurements via umbrella sampling. Our model experimental system is a bead fluctuating in a time-varying optical trap. We also show this for simulated force spectroscopy on a complex soft molecule—a piston-rotaxane. © *2012 American Institute of Physics.* [doi:10.1063/1.3680601]

I. INTRODUCTION

Soft matter is a sub-discipline of condensed matter physics that focusses upon chemical and biological matter that is easily deformed by thermal forces or fluctuations. Many examples of soft matter are entropy-dominated, i.e., they are characterized by many internal degrees of freedom and weak enthalpic interactions. Consequently, these soft materials or soft molecules can respond slowly in comparison to enthalpy-dominated systems. These long relaxation times can be problematic when trying to characterize the equilibrium states of soft matter, particularly in experiments where the external field is varied to access the states.

Here we demonstrate a method to extract equilibrium averages from experiments of soft matter that is not at equilibrium and in fact is driven out of equilibrium by the measurement. We experimentally demonstrate this with a simple optical tweezers experiment using a model soft system, a colloidal bead, and we extend this demonstration to a complex soft molecule, a piston-rotaxane that behaves as a molecular version of an automobile shock absorber, using simulated force spectroscopy.

The aim is to construct an equilibrium average of a property $\langle B \rangle_{eq}$ from an ensemble of non-equilibrium measures of B. Traditionally umbrella sampling is a technique where you more efficiently construct the average $\langle B \rangle_{eq}$ by using a biased ensemble, i.e., where each element of the ensemble is generated with a bias, u, but that bias is extracted in formulating the average using [1]

$$\langle B \rangle_{eq} = \frac{\langle B/u \rangle_u}{\langle 1/u \rangle_u}. \qquad (1)$$

Here $\langle \ \rangle_u$ represents an average over the biased ensemble and B/u is the measured property divided by the bias of that measurement. This is commonly used in equilibrium simulations where the region of equilibrium phase space over which B is dominant has a low probability of being sampled. In equilibrium umbrella sampling, the bias is applied synthetically (or en silico), usually through the Monte Carlo acceptance criteria; thus, umbrella sampling has been outside the interests of experimentalists. However, when Eq. (1) is used in the context of *dynamic* samples, it can be a valuable interpretative tool for experimentalists. Here we show that data from force spectroscopy of soft matter can be dynamically biased: quantifying and extracting that bias provides meaningful averages that characterize the soft system.

In non-equilibrium umbrella sampling, Eq. (1) is used to construct an equilibrium mean from an ensemble of dynamic or non-equilibrium trajectories of the system.[2–5] The system is initially at equilibrium and driven away from equilibrium as characterized by a parameter λ. Here we restrict ourselves to the case where the parameter externally controls the potential energy $\Phi(\mathbf{r}, \lambda)$, where $\mathbf{r}$ represents the system's configuration. An average of a property B, sampled at time t along the trajectories is a non-equilibrium mean that depends upon the protocol, that is the initial equilibrium state as well as the time-variation of the parameter, $\lambda(t)$. This non-equilibrium average, denoted by $\langle B \rangle_{\lambda(t), t}$ differs from the time-independent equilibrium average, $\langle B \rangle_{eq, \lambda(t)}$, that is obtained with a value of the potential fixed at $\lambda(t)$. Indeed, $\langle B \rangle_{\lambda(t), t}$ relaxes to the protocol-independent equilibrium average $\langle B \rangle_{eq, \lambda(t)}$—but for soft systems, the relaxation to this equilibrium average can be long. However, by Eq. (1), these non-equilibrium trajectories can yield an equilibrium average, without having to sample after a potentially long relaxation time. This is done by recognizing that the trajectories are biased

---

a)Author to whom correspondence should be addressed. Electronic mail: sevick@rsc.anu.edu.au.

according to

$$u = \exp[\beta w_t], \tag{2}$$

where w_t, the external work done on the system is

$$w_t = \int_0^t ds \dot{\lambda}(s) \frac{\partial \Phi(\mathbf{r}(s), \lambda(s))}{\partial \lambda}, \tag{3}$$

so that Eq. (1) is explicitly written for non-equilibrium umbrellas sampling as

$$\langle B \rangle_{eq,\lambda(t)} = \frac{\langle B \exp[-\beta w_t] \rangle_{\lambda(t),t}}{\langle \exp[-\beta w_t] \rangle_{\lambda(t),t}}. \tag{4}$$

This relation was first expressed by Crooks,[3] and more recently derived from deterministic mechanics by Williams and Evans.[4] See supplementary material for a brief review of that recent derivation.[6]

This non-equilibrium umbrella sampling [4,5] relates the equilibrium average of *any* measurable *state* property, B, to the work done in the measurement. In contrast, Jarzynski,[2] Crooks,[3] and others have used similar methods to determine the equilibrium free energy and potential of mean force [7] from non-equilibrium data. Jarzynski [8] has published a review that traces back some of the ideas that led to the non-equilibrium umbrella sampling method. Here we consider cases where B is a measured state property, accessible in experimental force spectroscopy using atomic force microscopy (AFM) or optical tweezers (OT). Both measurement techniques have been used in single molecule force spectroscopy; however, many of these measurements are not mechanically stable, resulting in discontinuities in the measured force, e.g., in the biomolecular unfolding transitions of order $\mathcal{O}(10-100)\, k_B T$. [9] This lack of mechanical stability means that the experimental bias, Eqs. (2) and (3), cannot be directly measured in experiment but must be inferred from models. Here we consider the non-equilibrium sampling method applied only to measurements that are mechanically stable.

II. EXPERIMENTAL FORCE SPECTROSCOPY OF A COLLOIDAL PARTICLE

We now consider the model experimental system: an optically trapped colloidal particle under a varying trap strength. In OT, a focussed Gaussian light beam creates a harmonic potential for the particle, $\Phi = \frac{1}{2}kx^2$ where x is the particle's position relative to the focal point and k is a trapping constant, controlled by altering the intensity of the laser. The particle's motion in a trap of constant strength, resolved over a fraction of a millisecond, is well described by an inertialess Langevin equation,

$$\xi \frac{dx}{dt} = -kx + g(t), \tag{5}$$

where ξ is a drag coefficient and $g(t)$ is the thermal force, a random force which follows a Gaussian distribution with zero mean $\langle g(t) \rangle = 0$, variance $\langle g(t)g(t') \rangle = 2k_B T \xi \delta(t - t')$. The relaxation time is determined by the decay of correlations in the particle position as $\tau = \xi/k$. Similar to that described in Ref. 10, we use a 4 W infrared laser ($\lambda = 1064$ nm) to trap a

$d = 5.5\, \mu$m polystyrene bead in water and calibrate by determining values of k and ξ from the power spectrum in accord with Eq. (5). To generate and measure dynamic particle trajectories, we vary the trap strength linearly whilst measuring the particle position, x. The trap strength is varied linearly in time from $k_0 \sim 1.4$ pN/μm to $k_1 \sim 4.7$ pN/μm at different rates, $\dot{k}$ spanning $1.3 - 130$ pN/(μm s), using a waveform generator in combination with an laser intensity controller. We simultaneously record the particle position by projecting the particle image onto a quadrant photodiode, sampling at 1 kHz with a resolution estimated to be ± 4 nm.[11] This protocol, illustrated in Figure 1, is automated and cycled several thousand times to create trajectories of the particle where $\dot{k} \equiv \dot{\lambda}$ is the protocol that determines the dynamic bias.

According to equipartition, a particle equilibrated in a harmonic trap of strength k fluctuates about the trap centre with mean square displacement (MSD) of $\langle x^2 \rangle_{eq} = k_B T/k$. However, the non-equilibrium MSD differs from this and depends upon the experimental protocol; we denote this non-equilibrium average as $\langle x^2 \rangle_{k(t), t}$. If the dimensionless confinement rate, $d^2 \dot{k}/k_B T$, is small compared with the relaxation rate of the system, k/ξ, then the particle's trajectories approach quasi-static behaviour where any average depends only upon the value of the trapping constant at that time t, or $\langle x^2 \rangle_{k(t), t}/(k_B T/k(t)) \rightarrow 1$. However, if the system is driven out of equilibrium, or the rate of trap tightening is fast compared with the relaxation time of the system, i.e., $\dot{k} \gg k_B T k/d^2 \xi$, then $\langle x^2 \rangle_{k(t), t}/(k_B T/k(t)) > 1$.

Figure 2 shows the non-equilibrium MSDs (open circles) of an optically trapped particle as a function of time for a set of trajectories initiated at k_0 and where the trap constant was increased at the fastest $\dot{k}$ over 25 ms. Here we normalize the non-equilibrium averages with the equipartition result, $k_B T/k(t)$. Notice that as the trajectory time increases from $t = 0$, $\langle x^2 \rangle_{k(t), t}/(k_B T/k(t))$ grows larger than 1, indicative of a system driven out of equilibrium with a confinement rate that is faster than the relaxation rate, or $\dot{k}/k(t) \gg k_B T/d^2 \xi$. However, as the trap is linearly tightened, the instantaneous relaxation rate, $k(t)/\xi$, increases linearly. Thus, at a later time the magnitude of $k(t)$ will be so large that the relaxation rate will exceed the constant confinement rate, meaning the particle response will be quasi-static with $\langle x^2 \rangle_{k(t), t}/(k_B T/k(t)) \rightarrow 1$ at later time. In Figure 2, the confinement rate is not sufficiently high and the protocol duration is not sufficiently long to see this return to quasi-static behaviour; however, a plateau is clearly evident. This plateau results because the system's relaxation towards equilibrium proceeds more quickly when the trap strength is stronger.

Associated with each trajectory is the accumulated work, i.e., the work done to more tightly confine the particle over a time t, or $w_t = \frac{1}{2} \int_0^t ds \, \dot{k}(s)x^2(s)$, by Eq. (3). Using the bias, Eq. (2), with Eq. (1) allows us to obtain expectation values for the equilibrium MSDs from the same non-equilibrium experiment. The results (closed data symbols) are shown in Figure 2. That $\langle x^2 \rangle_{eq, k(t)}/(k_B T/k(t)) \sim 1$ over the entire protocol time indicates that (i) the experimental measures of non-equilibrium particle positions are biased with the protocol-dependent weighting, Eq. (2), and (ii) that we are able to recover experimental estimates representative of
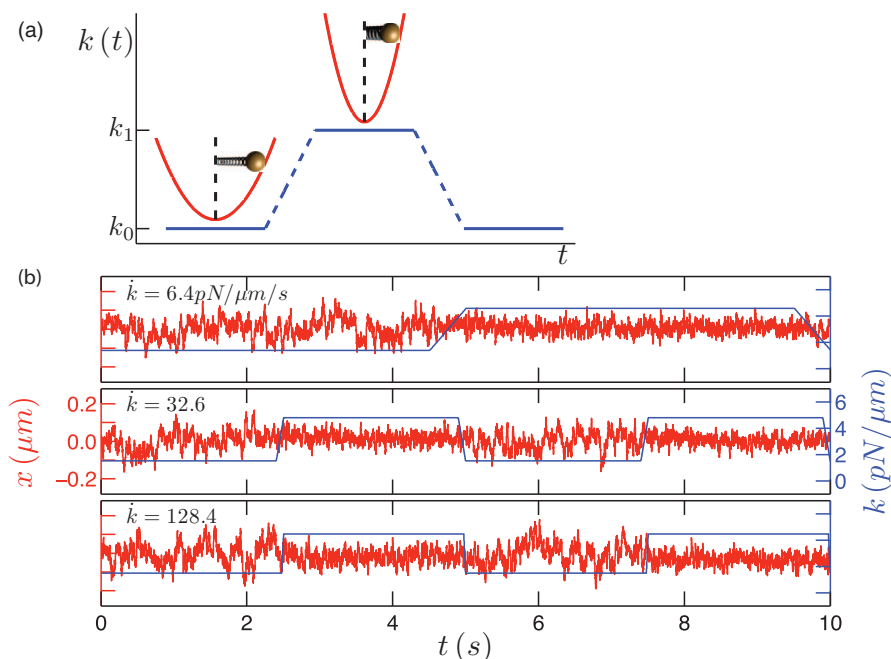
FIG. 1. (a) Schematic diagram of trap strength, k, versus t, illustrating the experimental protocol to generate non-equilibrium trajectories of a colloidal particle. The protocol involves cycling the trap strength between k_0, a weak trap where particle fluctuations are large, to k_1, a strong trap where fluctuations are reduced. (b) Experimental trace of particle's displacement from the trap centre versus time (red lines) against the time-dependent trapping strength, k (blue lines).

the equilibrium MSD. Also note that the error bars are $\sim$50% smaller in averages constructed with non-equilibrium umbrella sampling.

Next we consider the role of the protocol rate, specifically $\dot{k}$. Figure 3(a) compares the MSDs of an optically trapped particle at the end of the protocol (at time t_1), when the trap constant attains a fixed value, $k_1 = k(t_1)$, using various

confinement rates. The non-equilibrium average, $\langle x^2 \rangle_{k(t_1),t_1}$ (open circles), and equilibrium average that is determined from umbrella sampling, $\langle x^2 \rangle_{eq,k(t_1)}$ (filled circles), are determined from the same set of experimental trajectories at a given $\dot{k}$. Both are scaled by the equilibrium mean square displacement $\langle x^2 \rangle_{eq}$, which is determined experimentally by sampling the trajectory of a colloidal bead for 2 min at the fixed trap constant k_1. Fluctuations in these ratios are expected due to the finite number of non-equilibrium trajectories, as
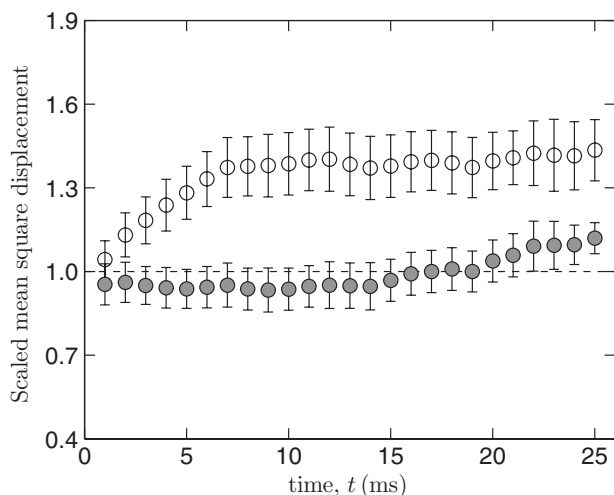

FIG. 2. Scaled MSD of an optically trapped particle versus time. The averages are constructed from a set of over 15 000 experimental trajectories where the trapping constant increases linearly in time, from k_0 to k_1 in $t = 25$ ms. The open symbols result from simple averages of particle positions along the non-equilibrium trajectories, or $\langle x^2 \rangle_{k(t),t}$ scaled by the expected equilibrium mean, $k_B T/k(t)$, where $k(t) = k_0 + \dot{k}t$. The filled symbols are similarly scaled averages constructed from umbrella sampling or $\langle x^2(t) \rangle_{eq,k(t)}$: that is, the mean is constructed from the same particle positions used in $\langle x^2 \rangle_{k(t),t}$, but where the non-equilibrium bias of each measure, Eq. (2), is removed. In this and other figures, the error in the mean corresponds to the standard deviation in data.
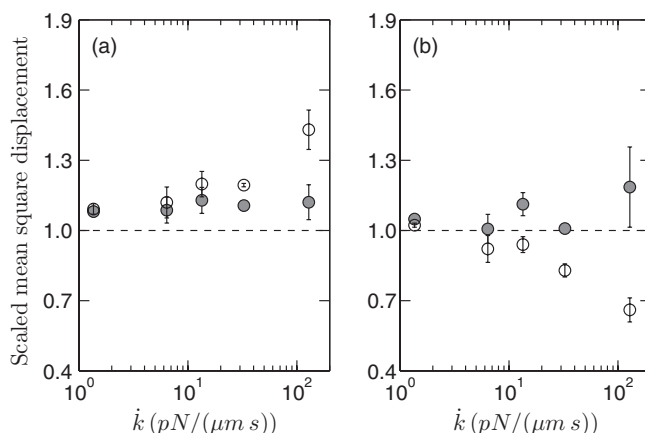
FIG. 3. Scaled MSD of an optically trapped particle at the completion of (a) confinement protocol and (b) release protocol at different protocol rates, $\dot{k}$. Open circles are scaled non-equilibrium averages, $\langle x^2 \rangle_{k(t),t}$, that depend strongly upon experimental protocol; filled circles are scaled equilibrium averages $\langle x^2 \rangle_{eq,k(t)}$, constructed using non-equilibrium umbrella sampling. All quantities are scaled by the experimentally determined equilibrium mean square displacement, $\langle x^2 \rangle_{eq}$, which by equipartition, $\langle x^2 \rangle_{eq} = k_B T/k$, is also used to determine the trap constant, k. These experimental averages are constructed from $7.8 - 16 \times 10^3$ experimental trajectories with k_0 of 1.3–1.5 pN/μm and k_1 between 4.5–4.8 pN/μm.

well as the temporal and spatial resolution of particle position measurements.

Figure 3(a) clearly shows that the scaled non-equilibrium average, $\langle x^2 \rangle_{k(t_1), t_1} / \langle x^2 \rangle_{eq}$, grows above unity with faster trap tightening. The mean constructed from umbrella sampling is expected to be independent of trap speed and match the equilibrium mean, that is, the filled circles should track the dotted line; but although $\langle x^2 \rangle_{eq, k(t_1)}$ differs from $\langle x^2 \rangle_{eq}$ by about 10%, this difference does not grow with or depend upon $\dot{k}$. That is, the umbrella sampling clearly eliminates the protocol dependence. This (the elimination of the protocol dependence) is even more evident when you consider the same mean quantities evaluated for $\dot{k} < 0$, where the trap loosens from k_1 to k_0 at different rates, Figure 3(b). The protocol dependence is evident in the non-equilibrium mean (open circles): this mean shrinks below unity as the traps loosens more quickly (as opposed to grows above unity as the trap tightens more quickly). In contrast, the mean constructed from umbrella sampling is (comparatively) independent of the direction and $\dot{k}$, showing protocol independence.

III. SIMULATED FORCE SPECTROSCOPY OF A PISTON-ROTAXANE MOLECULE

We now consider the non-equilibrium umbrella sampling method applied to force spectroscopy of a soft supramolecule, specifically the piston-rotaxane molecule, Fig. 4. A rotaxane is a molecule that is architecturally similar to some baby rattles: one or more ring-like molecules, threaded onto a molecular axle that is capped on both ends with large stoppers to prevent the rings, which slide on the axle, from falling off. The free rings provide translational entropy and, if the rings are few in number over a long axle, a significant molecular relaxation time. A piston-rotaxane is a rotaxane with one end of the axle fixed to a surface and the entropy of the free rings controlled by the top-most ring which is positioned with AFM or OT. As the free rings are analogous to a gas in a piston, and the top-most ring controls the length of axle (analogous to the volume of a piston), then we refer to the top-most ring as the piston-ring. This piston-rotaxane is predicted to behave as a scaled-down version of an automobile shock-absorber.[12] A version has already been synthesized and
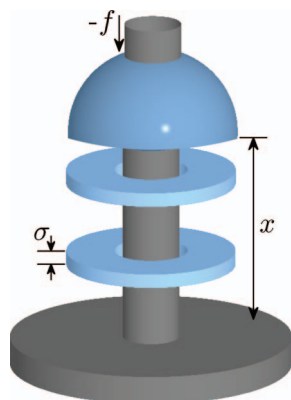

FIG. 4. Schematic of a piston-rotaxane molecule showing $N = 2$ free rings threaded onto an axle that is end-tethered to a surface. The top-most ring, referred to as a piston-ring, is optically trapped in force spectroscopy.

its force-extension profile measured using AFM;[13] however, that version contained no free rings and as such, it is missing the essential "gas" that imparts soft non-equilibrium properties. Equilibrium force profiles of a simple model of piston-rotaxanes as an entropy-dominated molecule have been predicted from classical partition functions.[12] These predictions yield an equilibrium average force, $\langle f(x) \rangle_{eq}$ on the piston ring as a function of position of the piston ring, x (which is equivalent to the available axle length), and the number of free rings, N. However, as these molecules are also predicted to have a long relaxation time, force spectroscopy will yield non-equilibrium force profiles.[14, 15]

As only a close analog of the piston-rotaxane has been synthesized, we resort to numerical solution of an stochastic equation of motion[14] to construct an ensemble of non-equilibrium trajectories of this optically manipulated supramolecule, Fig. 4. We consider the measured force on the piston ring as the molecule is compressed and expanded by optical tweezers. That is the external field driving the molecule out of equilibrium is the optical potential $\frac{1}{2}k(x - x_0)^2$ acting on the piston-ring where the optical trapping constant, k, is now constant, but the optical trap centre, x_0, is translated towards/away from the surface, causing the piston-ring to compress/expand the free rings. That is, the external control parameter is the trap centre translation, i.e., $\dot{\lambda} = \dot{x}_0$. The stochastic equation that models this OT experiment is simply Eq. (5), augmented by $f(x)$, the intermolecular force acting on the piston ring by the free rings,

$$\xi \frac{dx}{dt} = -k(x - x_0) + f(x) + g(t). \tag{6}$$

Commensurate with the energy, length, and time scales probed in optical tweezers based force spectroscopy, this time and position dependent intermolecular force is modeled using a coupled set of stochastic dynamics for the free rings, where non-conservative, hydrodynamic interactions are neglected and the same drag coefficient ξ is adopted for each of the free rings. See supplementary material for a review of this simple model,[6] originally described in Ref. 14, that we use for the responsive force, $f(x)$, of the entropy-dominated piston-rotaxane in Eq. (6) . It is possible to add more complex details to the model such as sophisticated ring–ring interactions or hydrodynamic interactions; however, this will not alter our aim and result. Our aim is to demonstrate that the bias in dynamic averages can be accounted for and extracted to obtain equilibrium averages and this is achieved independent of the particular dynamic model used. Moreover, the dynamical model here is used only in lieu of an existing molecule.

In force spectroscopy, the measurable property of interest is the force on the piston-ring, $f(t) = -k[x(t) - x_0(t)]$, or equivalently, in simulation, the piston-ring's time-dependent position in the trap, $x(t)$. Here we simulate dynamic trajectories and determine $f(t)$ or $x(t)$ at a time t after the trap centre has translated from $x_0(t = 0)$ with protocol rate $\dot{x}_0$, and from an ensemble of such trajectories we construct non-equilibrium mean force, $\langle f \rangle_{x_0(t), t}$. If the trap centre translation rate is small in comparison to the relaxation rate of the system (molecule + trapped piston-ring), then the trajectories are quasi-static

and the mean force is independent of protocol and identical to the equilibrium mean force $\langle f \rangle_{eq,x_0}$.

From simple physics, we can compare the molecule's relaxation rate, which depends upon the axle length (or amount of compression), x, and the number of free rings, N, with the controlled compression rate. For a piston-rotaxane with only $N = 1$ free ring, the relaxation time is simply the time that it takes for the free ring to diffuse the axle length available to it or $\tau_1 \sim \frac{x^2}{D} \sim \frac{x^2 \xi}{k_B T}$. The relaxation time for a piston-rotaxane with N free rings is thus $\tau_N \sim \frac{(x/N)^2}{D} \times N$. The imposed dimensionless compression rate is $\dot{x}_0/x$, so that the molecule's relaxation rate, relative to the compression rate, is $\frac{N k_B T}{x \dot{x}_0 \xi}$. Thus, we can expect quasi-static trajectories when we drive (compress) the system with a protocol rate $\dot{x}_0 \ll \frac{N k_B T}{x \xi}$. This provides an estimate that can be used in the design of soft piston-rotaxane molecules and their associated force measurements. Of course, this simplistic physical analysis can be refined by tallying time-correlation functions from numerical simulations of a particular dynamical model—or alternatively, by characterizing the soft molecules' dynamic response in an experimental force measurement. Associated with each trajectory is the accumulated work, i.e, the work done to compress or expand the piston-rotaxane over time t. This is, by Eq. (3) $w_t = \int_0^t ds \, \dot{x}_0 f(s)$, which used with Eq. (2) yields an equilibrium average.[16]

The role of protocol rate, or $\dot{x}_0$, on the mean force is shown in Fig. 5 for a compression and an expansion protocol. The non-equilibrium mean, $\langle f \rangle_{x_0(t),t}$ (open circles), and equilibrium mean determined from umbrella sampling, $\langle f \rangle_{eq,x_0(t)}$ (filled circles), are constructed from the same sets of simulated trajectories at a given $\dot{x}_0$. Both are scaled by the equilibrium force $\langle f \rangle_{eq}$, determined from equilibrium trajectories. Fluctuations in these ratios are minimal compared with the experimental ratios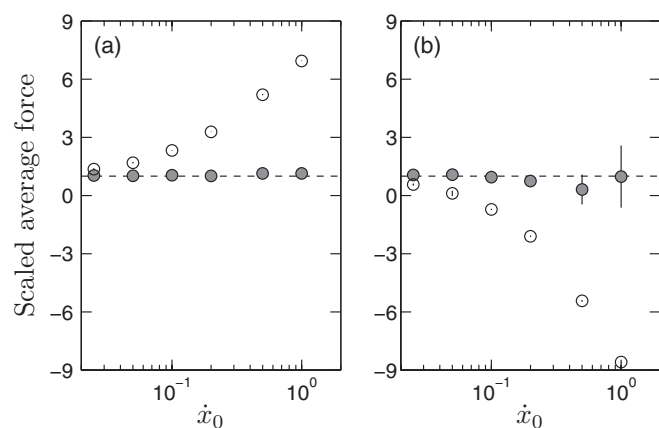 in Fig. 3 as (i) the number of simulated trajectories is considerably larger than the number of experimental ones, and (ii) the external field is controlled with a precision that is only limited by the numerical precision of the computer.

Figure 5(a) clearly shows that the scaled non-equilibrium mean, $\langle f \rangle_{x_0(t),t}/\langle f \rangle_{eq}$, grows with compression rate. This is of course the non-equilibrium property sought in the design of shock-absorbers: greater energy dissipation at higher compression rates. The mean constructed from umbrella sampling is independent of compression speed and matches the equilibrium mean, that is, the filled circles track the dotted line. The umbrella sampling clearly eliminates the history dependence of the trajectories from the average. This is even more evident when you consider the same mean quantities evaluated for the expansion of the molecular shock-absorber, Figure 3(b).

We have demonstrated the utility of non-equilibrium umbrella sampling in obtaining equilibrium information about soft systems with long relaxation times as compared with experimental measurement, specifically force spectroscopy. This technique should be particularly advantageous for the interpretation of force spectroscopy of soft systems, such as liposomes and membranes, that are driven out of equilibrium by the measurement itself, and have relaxation times comparable to or longer than the timescale of the experiment. Non-equilibrium averages from these measures reflect the experimental protocol as well as the system; but by extracting the dynamic bias from the data, we can generate equilibrium averages that characterize the system itself, and not the system plus experimental protocol. However, while we have focussed upon the average mean force, the technique can be applied to determine other mean properties of soft system which are perturbed from equilibrium, for example, the size of an elastic polymer from rheological measurement or the modulus of a membrane from force indentation.

FIG. 5. Scaled average force on the piston ring at the completion of (a) compression and (b) expansion protocol at different rates, $\dot{x}_0$ of an $N = 2$ piston rotaxane. Open circles are scaled non-equilibrium averages, $\langle f \rangle_{x_0(t),t}/\langle f \rangle_{eq}$; filled circles are scaled equilibrium averages constructed from non-equilibrium umbrella sampling, $\langle f \rangle_{eq,x_0(t)}/\langle f \rangle_{eq}$. All averages are scaled by the simulated equilibrium mean force, $\langle f \rangle_{eq}$ determined at the same fixed trap centre, $x_0(t)$. The compression/expansion rate is given by the speed of the optical trap centre, $\dot{x}_0$, where distance and time is in simulation units of ring thickness, d and the diffusion time for a ring to diffuse a distance equal to its thickness, or $d^2 \xi/(k_B T)$.

[1] D. Frenkel and B. Smit, *Understanding Molecular Simulation: From Algorithms to Applications*, 2nd ed. (Academic, San Diego, 2002).
[2] C. Jarzynski, Phys. Rev. E **56**, 5018 (1997).
[3] G. E. Crooks, Phys Rev E **61**, 2361 (2000).
[4] S. R. Williams and D. J. Evans, Phys. Rev. Lett. **105**, 110601 (2010).
[5] S. R. Williams, D. J. Evans, and D. J. Searles, J. Stat. Phys. **145**, 831 (2011).
[6] See supplementary material at http://dx.doi.org/10.1063/1.3680601 for a brief review of the derivation of Eq. (4) (see Appendix 1) and for a model of the responsive force of the piston-rotaxane (see Appendix 2).
[7] G. Hummer and A. Szabo, Proc. Natl. Acad. Sci. U.S.A. **98**, 3658 (2001).
[8] C. Jarzynski, *Annual Review of Condensed Matter Physics*, edited by J. S. Langer (Annual Reviews, Palo Alto, CA, 2011), Vol. 2, pp. 329–351.
[9] E. A. Shank, C. Cecconi, J. W. Dill, S. Marqusee, and C. Bustamante, Nature (London) **465**, 637 (2010).
[10] D. M. Carberry, J. C. Reid, G. M. Wang, E. M. Sevick, D. J. Searles, and D. J. Evans, Phys. Rev. Lett. **92**, 140601 (2004).
[11] Y. X. Gao and M. L. Kilfoil, Opt. Express **17**, 4685 (2009).
[12] E. M. Sevick and D. R. M. Williams, Langmuir **26**, 5864 (2010).
[13] B. Brough, B. Northrop, J. Schmidt, H. Tseng, K. Houk, J. F. Stoddart, and C. M. Ho, Proc. Natl. Acad. Sci. U.S.A. **103**, 8583 (2006).
[14] Y. X. Gao, D. R. M. Williams, and E. M. Sevick, Soft Matter **7**, 5739 (2011).
[15] Also, the measured response of these soft supramolecules depends upon the fluctuations of the optically trapped piston-ring. We note that the method of Hummer and Szabo (Ref. 7) could be used to obtain the potential of mean force, with no contribution due to the fluctuations of the optically trapped particle (piston-ring).
[16] Note that the equilibrium mean force is a different quantity to the potential of mean force focussed on by Hummer and Szabo (Ref. 7).